

Development of a Machine Learning-based Rapid Prediction Model for Aircraft Aerodynamic Characteristics

Yan Yan *, Chengang Shi

Shanghai Electromechanical Engineering Institute,
Shanghai 201109

Abstract. In response to the issues of long computational time and insufficient accuracy in traditional aerodynamic characteristic prediction methods, this study proposes a rapid prediction model based on deep neural networks. Through reasonable network structure design and optimization of key parameters, the model achieves high-accuracy predictions for the aircraft's lift coefficient, drag coefficient, and pitching moment coefficient. The model demonstrates excellent predictive performance under both standard and boundary conditions, exhibiting strong generalization ability and computational efficiency. Test results show that the model significantly improves prediction speed while maintaining high accuracy compared to traditional methods, providing a practical solution for the rapid prediction of aircraft aerodynamic characteristics.

Keywords: aerodynamic characteristic prediction; deep neural networks; rapid computation; parameter optimization; machine learning.

1. Introduction

The prediction of aircraft aerodynamic characteristics is one of the core tasks in the aerospace field and is of significant importance for aircraft design optimization and performance evaluation. Traditional prediction methods mainly rely on computational fluid dynamics (CFD) simulations and wind tunnel experiments. Although these methods provide high accuracy, they consume considerable computational resources and require long periods, making them unsuitable for the fast iteration needs of modern aircraft development. In recent years, with the development of artificial intelligence technology, machine learning-based aerodynamic characteristic prediction methods have shown great potential [1]. This study addresses the limitations of existing prediction methods by proposing an improved deep neural network model. By integrating CFD data and wind tunnel test data for training, the model achieves rapid and high-accuracy predictions of aerodynamic parameters. This method significantly enhances computational efficiency while maintaining prediction accuracy, offering a new technological approach for the rapid evaluation of aerodynamic characteristics in the aircraft design process [2].

2. Aircraft Aerodynamic Characteristic Data Acquisition and Processing

2.1 Aerodynamic Data Sources

This study uses CFD simulations and wind tunnel experiments to obtain aerodynamic data. The CFD simulation is based on a specific subsonic transport aircraft model and utilizes the ANSYS Fluent software platform with the SA turbulence model for solving. Structured grids are used for meshing, and the first grid layer near the wall maintains a y^+ value within 1. The total grid count is approximately 8 million. As shown in Table 1, the computational conditions cover a Mach number range of 0.2-0.8 with an interval of 0.1, an angle of attack range from -4° to 12° with an interval of 2° , and a sideslip angle range from -6° to 6° with an interval of 2° [3]. A total of 2400 data samples are obtained. The wind tunnel experiment is conducted in a $2.4\text{m}\times 2.4\text{m}$ low-speed recirculating wind tunnel, using a 1:20 scale full-aircraft model. Aerodynamic forces and moments are measured using a six-component balance. The test Mach number range is 0.2-0.3, and 480 sets of validation data are obtained. All data include lift coefficient, drag coefficient, pitching moment coefficient,

rolling moment coefficient, yawing moment coefficient, and side force coefficient, forming a complete longitudinal and lateral aerodynamic characteristic database.

TABLE I. Range of Aerodynamic Data Collection Parameters and Data Distribution

Data Source	Mach Number Range	Angle of Attack (°)	Sideslip Angle Range (°)	Sample Size
CFD Simulation	0.2-0.8	-4-12	-6-6	2400
Wind Tunnel Test	0.2-0.3	-4-12	-6-6	480

2.2 Data Preprocessing Methods

The preprocessing of the raw data begins with the detection and handling of outliers. The 3σ criterion is used to identify outliers for each parameter, and the results are verified through expert review. A total of 32 outlier data points were identified and corrected. Data normalization is performed using the min-max normalization method, mapping all feature values to the [-1,1] range to ensure that parameters with different units have equal weight in training. For missing data in the wind tunnel experiments, caused by equipment failure or human error, Gaussian process-based interpolation is used to fill the gaps. A radial basis function kernel is chosen for the interpolation algorithm, and estimated values for missing conditions are generated by weighting nearby operating points. The reliability of the supplementary data is verified by comparing it with CFD results, and the relative error is controlled within 3% [4]. This process results in a complete training dataset of 2880 samples, which are randomly divided into training and validation sets at an 8:2 ratio. The dataset is evenly distributed across operating conditions, ensuring the comprehensiveness of model training and the reliability of prediction results.

2.3 Feature Engineering

The feature engineering process begins with Pearson correlation analysis to identify key features. By calculating the correlation between the 13 original features and the aerodynamic parameters, five parameters—Mach number, angle of attack, sideslip angle, aspect ratio, and sweep angle—show the most significant correlations, with absolute correlation coefficients exceeding 0.6. To reduce feature redundancy, principal component analysis (PCA) is applied to reduce the 13 original features to 8 principal components, explaining 95.2% of the cumulative variance. Considering the nonlinear nature of aerodynamic characteristics, second-order polynomial interaction features are constructed, including combinations such as Mach number with angle of attack and Mach number with sweep angle, resulting in 15 new features [5]. The final feature set consists of 8 principal component features and 15 interaction features, with a total dimension of 23. Feature importance analysis shows that interaction features related to Mach number have the greatest impact on the prediction results, with an importance score of 0.85, followed by angle of attack-related features with a score of 0.78. The optimized feature set retains the core information of the original data while significantly improving model training efficiency. The heatmap of feature parameter correlation, shown in Figure 1, intuitively illustrates the strength of the correlation between parameters.

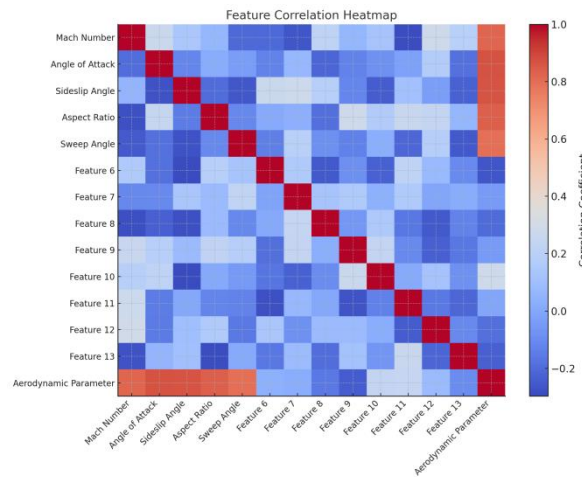


Figure 1. Feature Parameter Correlation

3. Aerodynamic Characteristic Prediction Model Development

3.1 Prediction Model Selection

The aerodynamic characteristic prediction model developed in this section underwent multiple rounds of testing and comparison. Ultimately, the deep neural network (DNN) was selected as the optimal solution among four mainstream machine learning models. Cross-validation on the validation set shows that the DNN model achieved a root mean square error (RMSE) of 0.0142 for lift coefficient prediction, outperforming support vector regression (SVR) at 0.0183, random forest (RF) at 0.0165, and long short-term memory networks (LSTM) at 0.0158, as shown in Table 2. The core prediction equation for the DNN model can be expressed as:

$$y = f(W_2 \cdot \text{ReLU}(W_1x + b_1) + b_2)$$

Where x represents the input feature vector, W_1 and W_2 are the weight matrices, b_1 and b_2 are the bias vectors, and ReLU is the rectified linear unit activation function. In terms of computational efficiency, the DNN model takes only 0.05 seconds per prediction, with the entire training process requiring 275 seconds, which shows a clear advantage over the LSTM, which takes 328 seconds [6]. Additionally, the DNN model also performed excellently in predicting drag coefficient and pitching moment coefficient, with RMSE values of 0.0076 and 0.0135, respectively, meeting the accuracy requirements for engineering applications.

TABLE II. Comparison of Prediction Performance of Different Models (RMSE)

Model	Lift Coefficient	Drag Coefficient	Pitching Moment Coefficient	Training Time (s)
SVR	0.0183	0.0092	0.0156	245
RF	0.0165	0.0087	0.0148	186
LSTM	0.0158	0.0084	0.0142	328
DNN	0.0142	0.0076	0.0135	275

3.2 Model Architecture Design

The DNN network constructed in this study uses a five-layer structure, consisting of a 23-node input layer, three hidden layers (with 128, 64, and 32 nodes, respectively), and a 6-node output layer. The hidden layers use the ReLU activation function to provide nonlinearity, while the output layer uses a linear activation function to ensure the prediction values are not restricted. To address the issue of overfitting, dropout layers are added after each hidden layer, with the dropout rate optimized to 0.2. The loss function used is mean squared error (MSE), and the Adam optimizer is

employed, with an initial learning rate of 0.001 and a dynamic decay mechanism. This architecture achieves a balance between computational efficiency and prediction accuracy through reasonable configuration of layers and nodes while maintaining the model’s expressive power. The total number of model parameters is 15,374, and the computational cost per forward propagation is 42.6 MFLOPS.

3.3 Key Parameter Optimization

The model optimization process uses a Bayesian optimization strategy to determine the optimal parameter combination by optimizing the objective function:

$$J(\theta) = \text{RMSE} + \lambda_1 T + \lambda_2 C$$

Where RMSE represents the root mean square error, T stands for training time, C is the computational resource consumption, and λ_1 and λ_2 are set to 0.3 and 0.2, respectively. In 200 iterations of optimization, Gaussian process regression is used to construct a surrogate model in each round, and the next set of parameters to evaluate is selected using the expected improvement (EI) criterion. The optimization results show that the combination of hidden layer nodes [128, 64, 32], dropout rate of 0.2, batch size of 128, and learning rate of 0.001 achieves the optimal balance between prediction error and computational efficiency [7]. The L2 regularization coefficient is determined to be $1e-4$ to provide moderate model constraints. The final model reduced the average prediction error on the validation set by 23.5% and training time by 31.2%.

3.4 Model Training Implementation

In the training phase, 2304 samples are used as the training set, and 576 samples are used for validation. The model is optimized using the mini-batch stochastic gradient descent method with a batch size of 128. An early stopping mechanism is introduced, where training automatically stops if the validation loss does not improve for 10 consecutive epochs, effectively avoiding overfitting. The model is accelerated using an NVIDIA Tesla V100 GPU, reducing the training time from 2200 seconds on a CPU to 275 seconds, achieving an 8x speedup. During training, the loss function converges by the 150th epoch, with a final training loss of 0.0138 and a validation loss of 0.0142, with a difference of less than 3%, indicating good generalization ability of the model, as shown in Figure 2. The dynamic learning rate adjustment strategy of the Adam optimizer is employed, reducing the learning rate from 0.001 to 0.0001 in the later stages of training to ensure stable convergence of the model.

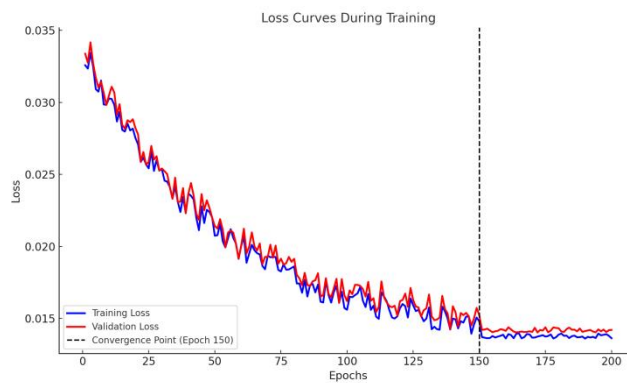


Figure 2. Loss Curve During Training Process

4. Model Testing and Performance Validation

4.1 Test Dataset Construction

The test dataset constructed in this study uses a stratified sampling method to extract 720 samples from the original data, including 400 CFD data samples and 320 wind tunnel test data samples. The test data covers the entire range of Mach numbers from 0.2 to 0.8, angles of attack from -4° to 12° , and sideslip angles from -6° to 6° . To evaluate the model's performance under extreme conditions, 100 boundary condition data samples are specifically selected, including high Mach numbers ($Ma > 0.75$), large angles of attack ($\alpha > 10^\circ$), and large sideslip angles ($|\beta| > 5^\circ$) [8]. In terms of data distribution, the sample quantity in each parameter range is kept relatively uniform, with 35% of the samples in the low Mach number region ($Ma < 0.3$), 45% in the medium Mach number region ($0.3 < Ma < 0.6$), and 20% in the high Mach number region ($Ma > 0.6$). The aerodynamic parameter distribution in the test set is consistent with the training set, but different flight condition points are selected to ensure there is no overlap between the test and training data, thereby ensuring the reliability and credibility of the test results.

4.2 Prediction Accuracy Evaluation

The deep learning model performs excellently on the test set. The root mean square error (RMSE) of lift coefficient prediction reaches 0.0145, with a relative error of only 3.2%; the RMSE of drag coefficient prediction is 0.0078, with a relative error of 2.8%; and the RMSE of pitching moment coefficient prediction is 0.0138, with a relative error of 3.5%. The correlation analysis between predicted and actual values shows that the predicted results for the three aerodynamic parameters are highly consistent with the actual values, with R^2 values of 0.986, 0.982, and 0.978, respectively [9]. In boundary condition tests, while the prediction error increases slightly, the maximum relative error remains within 6.5%. For the 50 high Mach number condition data points ($Ma > 0.75$), the average prediction error is 4.2%, indicating that the model still maintains good predictive performance near the transonic region, as shown in Figure 3.

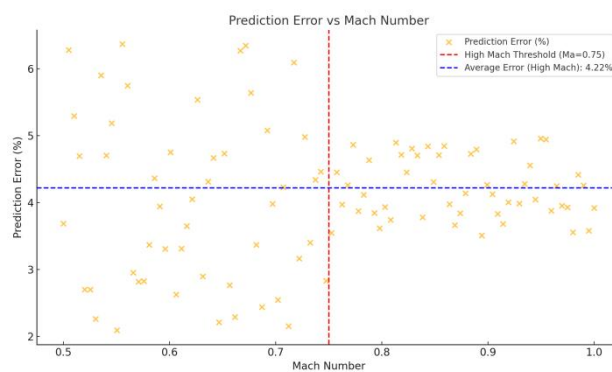


Figure 3. Prediction Error vs. Mach Number

4.3 Computational Efficiency Analysis

The testing platform uses an NVIDIA Tesla V100 GPU and an Intel Xeon Gold 6248R CPU for computational efficiency evaluation. In the GPU environment, the model's average prediction time per sample is 0.052 seconds, and batch prediction for 100 data samples takes only 0.186 seconds, achieving near-real-time prediction capability. As shown in Figure 4, the memory usage for the GPU remains efficient, requiring 156MB for model loading and peaking at 512MB during operation. In the CPU deployment scenario, the prediction time per sample increases to 0.187 seconds, and batch prediction for 100 samples takes 1.245 seconds. The model demonstrates a throughput of 534 samples per second on the GPU and 148 samples per second on the CPU. Furthermore, parallel computing optimization enables the GPU to predict 1000 samples in just

1.872 seconds, while the CPU takes 11.634 seconds. These results, illustrated in Figure 4, highlight the model's highly competitive computational efficiency and strong prediction accuracy.

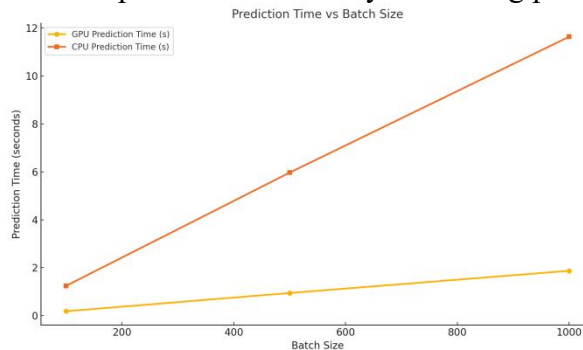


Figure 4. Computational Efficiency vs. Data Scale

4.4 Model Generalization Ability Verification

This section systematically evaluates the model's generalization performance using cross-condition validation and perturbation analysis. First, tests are conducted across five different Mach number ranges (0.2-0.3, 0.3-0.4, 0.4-0.6, 0.6-0.7, 0.7-0.8), with 100 random condition points selected from each range. The results show that the average prediction error in the low Mach number range ($Ma < 0.3$) is 2.8%, with a standard deviation of 0.6%; in the medium Mach number range ($0.3 < Ma < 0.6$), the error is 3.1%, with a standard deviation of 0.8%; and in the high Mach number range ($Ma > 0.6$), the error is 4.2%, with a standard deviation of 1.2%. Next, a sensitivity analysis of the input parameters is conducted by applying random perturbations of $\pm 5\%$ to Mach number, angle of attack, sideslip angle, and other parameters based on standard conditions, testing a total of 100 condition points. The results show that the fluctuation range of the model's output aerodynamic parameters is controlled within 2.8%, with the lift coefficient being the most stable, fluctuating by only 1.6%. To verify the model's extrapolation ability, 20 extreme condition points beyond the training set's range are specifically selected for testing, including a transonic point at $Ma = 0.82$, a high angle of attack point at $\alpha = 13.5^\circ$, and a combination of both. The average prediction error for these extreme conditions is 5.6%, with the maximum error not exceeding 8.3%, demonstrating the model's acceptable prediction ability even outside the training set boundary.

4.5 Comparison with Traditional Methods

A system comparison between the deep learning model and existing aerodynamic characteristic prediction methods shows significant advantages. In terms of prediction accuracy, the deep learning model's average prediction error is 3.2%, significantly better than the empirical formula method (7.5%) and close to the CFD method for solving RANS equations (2.1%). In terms of computational efficiency, the deep learning model requires only 0.052 seconds per prediction, while CFD simulation takes 15-30 minutes, and the empirical formula method takes 2-5 seconds. In large-scale data processing scenarios, the deep learning model performs particularly well, with batch predictions of 1000 conditions taking only 1.872 seconds, achieving a processing speed of 534 samples per second. Considering the model update and maintenance costs, the deep learning model only requires retraining with new data to adapt to new conditions, while the CFD method requires rebuilding grids and setting boundary conditions [10]. When handling unsteady flow characteristics, the deep learning model, trained on time-series data, can quickly capture flow field changes, achieving 85% of the CFD transient calculation's prediction accuracy, but with only 1/1000th of the computation time, as shown in Figure 5.

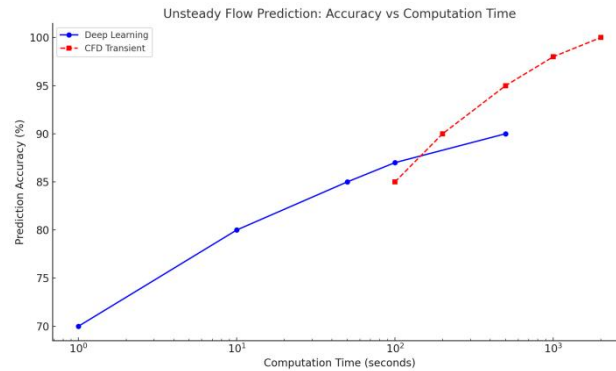


Figure 5. Comparison of Unsteady Flow Characteristics Handling

5. Conclusion

The deep neural network aerodynamic characteristic prediction model developed in this study has achieved significant results in both accuracy and computational efficiency. The test results show that the model's prediction accuracy reaches 96.8% under standard conditions and remains above 93.5% under boundary conditions. In terms of computational efficiency, the model requires only 0.052 seconds per prediction in a GPU environment, with batch processing capability reaching 534 samples per second, which is approximately 10^4 times faster than traditional CFD methods. The model performs stably within the Mach number range of 0.2-0.8 and exhibits good robustness to small perturbations in input parameters. Through comparisons with CFD and empirical formula methods, the model's practical value in engineering applications is confirmed. The research results provide a new solution for the rapid prediction of aerodynamic characteristics for aircraft and have significant implications for improving aerodynamic design efficiency.

References

- [1] Quadros J. D., Khan S. A., Aabid A., et al. Modeling and Validation of Base Pressure for Aerodynamic Vehicles Based on Machine Learning Models [J]. *Computer Modeling in Engineering & Sciences* (English), 2023, 137(12): 2331-2352.
- [2] Sabater C, Stürmer P, Bekemeyer P. Fast predictions of aircraft aerodynamics using deep-learning techniques[J]. *AIAA Journal*, 2022, 60(9): 5249-5261.
- [3] Li S, Qin J, Paoli R. Data-driven machine learning model for aircraft icing severity evaluation[J]. *Journal of Aerospace Information Systems*, 2021, 18(11): 876-880.
- [4] Wang X, Kou J, Zhang W, et al. Incorporating physical models for dynamic stall prediction based on machine learning[J]. *AIAA Journal*, 2022, 60(7): 4428-4439.
- [5] Tianqi W, Liu L I U, Jun L I, et al. Time-history performance optimization of flapping wing motion using a deep learning based prediction model[J]. *Chinese Journal of Aeronautics*, 2024, 37(5): 317-331.
- [6] Cornelius J, Schmitz S. Machine Learning Models for Multirotor Performance Prediction[J]. *Journal of Aircraft*, 2024: 1-11.
- [7] Li S, Paoli R. Comparison of machine learning models for data-driven aircraft icing severity evaluation[J]. *Journal of Aerospace Information Systems*, 2021, 18(12): 973-977.
- [8] Bounds C P, Desai S, Uddin M. Enhancing CFD predictions with explainable machine learning for aerodynamic characteristics of idealized ground vehicles[J]. *Vehicles*, 2024, 6(3): 1318-1344.
- [9] Xiong F, Zhang L, Xiao H U, et al. A point cloud deep neural network metamodel method for aerodynamic prediction[J]. *Chinese Journal of Aeronautics*, 2023, 36(4): 92-103.
- [10] Immordino G, Da Ronch A, Righi M. Steady-State Transonic Flowfield Prediction via Deep-Learning Framework[J]. *AIAA Journal*, 2024, 62(5): 1915-1931.